BJP British Journal of Pharmacology

DOI:10.1111/bph.12972
www.brjpharmacol.org

RESEARCH PAPER

Diadenosine tetraphosphate induces tight junction disassembly thus increasing corneal epithelial permeability

Correspondence
Dr Jesús Pintor, Department of Biochemistry and Molecular Biology IV, Faculty of Optics and Optometry, Universidad Complutense Madrid, C/Arcos de Jalón 118, 28037 Madrid, Spain.
E-mail: jpintor@ucm.es

Received
26 May 2014
Revised
26 September 2014
Accepted
29 September 2014

P Loma, A Guzman-Aranguez, M J Pérez de Lara and J Pintor

Department of Biochemistry and Molecular Biology IV, Faculty of Optics and Optometry, Universidad Complutense de Madrid, Spain

BACKGROUND AND PURPOSE

Here, we have studied the effects of the dinucleotide P^1, P^4-Di (adenosine-5′) tetraphosphate (Ap_4A) on corneal barrier function conferred by the tight junction (TJ) proteins and its possible involvement in ocular drug delivery and therapeutic efficiency.

EXPERIMENTAL APPROACH

Experiments *in vitro* were performed using human corneal epithelial cells (HCLEs) treated with Ap_4A (100 μM) for 5 min. Western blot analysis and transepithelial electrical resistance (TEER) were performed to study the TJ protein levels and barrier function respectively. Intracellular pathways involved were determined using an ERK inhibitor and $P2Y_2$ receptor siRNAs. In *in vivo* assays with New Zealand rabbits, TJ integrity was examined by zonula occludens-1 (ZO-1) staining. The hypotensive compound 5-methoxycarbonylamino-N-acetyltryptamine (5-MCA-NAT) was used to assess improved delivery, measuring its levels by HPLC and measuring intraocular pressure using 5-MCA-NAT, P2Y receptor antagonists and $P2Y_2$ siRNAs.

KEY RESULTS

Two hours after Ap_4A pretreatment, TJ protein levels in HCLE cells were reduced around 40% compared with control. TEER values were significantly reduced at 2 and 4 h (68 and 52% respectively). TJ reduction and ERK activation were blocked by the ERK inhibitor U012 and $P2Y_2$ siRNAs. *In vivo*, topical application of Ap_4A disrupted ZO-1 membrane distribution. 5-MCA-NAT levels in the aqueous humour were higher when Ap_4A was previously instilled and its hypotensive effect was also increased. This action was reversed by P2Y receptor antagonists and $P2Y_2$ siRNA.

CONCLUSIONS AND IMPLICATIONS

Ap_4A increased corneal epithelial barrier permeability. Its application could improve ocular drug delivery and consequently therapeutic efficiency.

Abbreviations

5-MCA-NAT, 5-methoxycarbonylamino-*N*-acetyltryptamine; Ap_4A, P^1, P^4-Di (adenosine-5′) tetraphosphate; HCLE, human corneal epithelial cells; IOP, intraocular pressure; NGS, normal goat serum; PPADS, pyridoxal phosphate-6-azo (benzene-2′,4′-disulfonic acid); RB2, reactive blue 2; TEER, transepithelial electrical resistance; TJ, tight junctions; U0126, 1,4-diamino-2,3-dicyano-1,4-bis (o-aminophenylmercapto) butadiene ethanolate; ZO-1, zonula occludens-1

Tables of Links

TARGETS
Enzyme[a]
ERK1/2
GPCR[b]
$P2Y_2$ receptor

LIGANDS
Ap_4A, diadenosine tetraphosphate
PPADS, pyridoxal phosphate-6-azo (benzene-2′,4′-disulfonic acid)
RB2, reactive blue 2
Suramin
U0126
UTP, uridine triphosphate

These Tables list key protein targets and ligands in this article which are hyperlinked to corresponding entries in http://www.guidetopharmacology.org, the common portal for data from the IUPHAR/BPS Guide to PHARMACOLOGY (Pawson *et al.*, 2014) and are permanently archived in the Concise Guide to PHARMACOLOGY 2013/14 ([a,b] Alexander *et al.*, 2013a,b).

Introduction

Diseases affecting both the ocular surface as well as the anterior eye segment are mostly treated by topically administered drugs. However, ocular drug delivery is extraordinarily limited by the defensive barriers of the eye resulting in poor drug bioavailability (Kompella *et al.*, 2010). A key barrier encountered by drugs is the corneal epithelium on the ocular surface that restricts the entrance of pathogen and potentially harmful substances protecting the eye, but also limiting drug absorption. Corneal epithelial cells are connected to each other through intercellular junctions that form an epithelial junctional complex formed by tight junctions (TJs), adherens junctions and desmosomes (Ban *et al.*, 2003). All of them are necessary for the maintenance of this epithelial barrier. TJ are multifunctional and dynamic protein complexes that connect adjacent cells by sealing the intercellular space between cells preventing the paracellular movement of solutes, ions and water. The protein components of TJs are mainly formed by transmembrane proteins such as occludin (Furuse *et al.*, 1993), claudins (Mineta *et al.*, 2011), junctional adhesion molecules (Martin-Padura *et al.*, 1998) and cytoplasmic scaffolding proteins like the zonula occludens protein family (Wittchen *et al.*, 1999). In particular, zonula occludens-1 (ZO-1), occludin and claudins are expressed in the cornea and play a key role in the barrier function (Ban *et al.*, 2003; Sosnova-Netukova *et al.*, 2007; Yoshida *et al.*, 2009).

Epithelial TJs and, therefore, the paracellular permeability are controlled by a considerable variety of agents and molecules including matrix metalloproteinases (Pflugfelder *et al.*, 2005), cytokines (Petecchia *et al.*, 2012), growth factors (Hollande *et al.*, 2001) and hormones (Sadowska *et al.*, 2010). Effects of these different molecules on TJ barrier function are mediated by second messengers such as cAMP (Adamson *et al.*, 1998), Ca^{2+} (Brown and Davis, 2002), diacylglycerol (Balda *et al.*, 1993) and signalling pathways such as Rho/ROCK (Stamatovic *et al.*, 2006), PKC (Ivanov *et al.*, 2009) PKA (Klingler *et al.*, 2000) and MAPK pathways (Basuroy *et al.*, 2006; Cohen *et al.*, 2010). These diverse transduction pathways can affect the TJ assembly and function through a variety of mechanisms including the regulation of TJ protein expression at the transcriptional level or by endocytosis as well as regulating TJ protein function by posttranslational mechanisms such as phosphorylation (Harhaj and Antonetti, 2004).

Interestingly, some of these intracellular signalling pathways regulating TJ barrier function may be associated in some tissues with the stimulation of metabotropic type purinergic receptors (P2Y). These receptors have been described on the ocular surface in structures like cornea, conjunctiva and also in other ocular locations such as the ciliary body, trabecular meshwork and retina (Guzman-Aranguez *et al.*, 2013). P2Y receptors are activated by nucleotides as well as dinucleotides. Within these molecules, dinucleotides and, in particular, diadenosine tetraphosphate (Ap_4A) have special relevance in the eye (Guzman-Aranguez *et al.*, 2007; 2011). Ap_4A is present as an active component of ocular secretions such as tears and aqueous humour (Pintor *et al.*, 2002b; 2003b), and it can activate P2Y purinergic receptors localized on the ocular surface and the anterior segment. Several biochemical and physiological roles have been proposed for Ap_4A in the eye. These include the control of processes such as induction of tear secretion, lysozyme production, acceleration of corneal wound healing and modulation of intraocular pressure (IOP) (Pintor *et al.*, 2002a; Soto *et al.*, 2005; Mediero *et al.*, 2008; Peral *et al.*, 2008). Little is known about the contribution of Ap_4A to other processes such as the regulation of ocular barrier permeability.

Taking into account the pivotal role of corneal epithelium as a limiting barrier for drug absorption, the study of the corneal epithelial barrier regulation is a key subject to improve the ocular penetration of topically applied drugs into the eye. With this aim, in this study we have investigated the effect of Ap_4A on the TJ corneal epithelial barrier function, determining the intracellular mechanisms involved in this effect. Moreover, taking advantage of the effect induced by Ap_4A on TJ protein levels and function and subsequently in corneal epithelial permeability, we have used this dinucleotide to enhance the delivery of hypotensor drugs into the eye.

Methods

In vitro *assays*

Cell culture. Telomerase-immortalized human corneal epithelial cells (HCLE) were used for the experiments and were generously provided by Dr. Ilene Gipson (Gipson *et al.*, 2003). Cells were cultured in keratinocyte serum-free medium (K-SFM) (Invitrogen) supplemented with 0.4 mM $CaCl_2$, 25 $\mu g \cdot mL^{-1}$ bovine pituitary extract, 0.2 $ng \cdot mL^{-1}$ EGF and 1% penicillin–streptomycin. Cells were incubated and maintained in a humidified chamber with 5% CO_2 at 37°C and 95% humidity until confluence. HCLE cells were treated with the dinucleotide Ap_4A (100 μM) for a period of 5 min. This time was chosen as it is the maximal time that any compound can remain on the ocular surface before it is totally drained by the lachrymal point (Lang, 1995). After nucleotide removal, cells were studied at different times (1, 2, 6 and 24 h), and TJ protein levels and phosphorylation status of ERK1/2 were evaluated by Western blot analysis. Likewise, TJ function was analysed by transepithelial electrical resistance (TEER).

Protein isolation and Western blot analysis. Cells were lysed using RIPA buffer (150 mM NaCl, 25 mM Tris HCL pH 7.6, 1% Nonidet P-40, 1% sodium deoxycholate, 0.1% SDS) and supplemented with Protease Inhibitor Cocktail Kit (Thermo Scientific, Rockford, IL, USA). The collected cell lysates were centrifuged at 20 000 x *g* for 15 min at 4°C. Protein concentration was determined using the bicinchoninic acid protein assay reagent kit (Pierce, Rockford, IL, USA). Samples were diluted in Laemmli buffer, separated by electrophoresis SDS-PAGE and transferred to nitrocellulose membranes. Then, membranes were incubated with blocking solution containing 5% non-fat dry milk diluted in PBS 1× for 1 h at room temperature and then incubated with primary antibodies (rabbit anti-ZO-1 (1:500), rabbit anti-occludin (1:100), rabbit anti-claudin-7 (1:100), rabbit anti-$P2Y_2$ receptor (1:1000) and anti-pERK (1:1000) overnight at 4°C. After washing, blots were incubated with peroxidase-conjugated secondary antibodies (1:10 000) for 1 h at room temperature. Mouse monoclonal anti-GAPDH (1:500) and ERK2 (1:500) antibodies served as a loading control. Films were scanned and a densitometric analysis was performed using Kodak molecular imaging software (Kodak, Rochester, NY, USA). Data were normalized by GAPDH, and the value of the ratio protein/GAPDH for the control was defined as 100%. In the case of ERK1/2 phosphorylation, data were normalized by ERK2 protein levels. All data shown are representative of three independent experiments.

Intracellular pathways and siRNA assays. Intracellular pathways mediating Ap_4A effect were determined using $P2Y_2$ siRNAs and ERK inhibitors (U0126). For assays with siRNA against $P2Y_2$ receptors, cells were transfected at 50% confluence. A mixture of two individual sequences (5′-CAA CAU GGC CUA CAA GGU UUU-3′ and 5′-GAA CUG ACA UGC AGA GGA UUU-3′) previously described (Boucher *et al.*, 2010) were used. A final concentration of 50 nM siRNA (per every siRNA sequence) was transfected using JetPRIME reagent according to the manufacturer's protocol. The transfection media were replaced by cell growth medium after 4 h post transfection, and the cells were cultured for 48 h prior to experimentation. This period of time as well as siRNA concentration was previously optimized in preliminary experiments.

For assays with the ERK inhibitor U0126 (100 μM), HCLE cells were pre-incubated for 30 min. After that, in the presence of the inhibitor, Ap_4A (100 μM) was added for 5 min. Following nucleotide removal, cells were incubated for 2 h and TJ protein levels and phosphorylation status of ERK1/2 were analysed by Western blot.

Immunocytochemistry. For immunocytochemical detection of ZO-1, HCLE cells were cultured to confluence in K-SFM medium in four chamber slides. Then HCLEs were separately treated with Ap_4A and uridine triphosphate (UTP) in doses of 100 μM for 5 min. After the nucleotides were removed and fresh medium wash was added, cells were incubated for 2 h, then washed with 1× PBS and fixed with 4% PFA for 15 min. After washing, cells were permeabilized with PBS 1× Triton X-100 and incubated with blocking buffer for 1 h at room temperature and then stained with the primary antibody rabbit anti-ZO-1 (1:125) diluted in PBS 1× 0.1% Triton X-100 overnight. Then, FITC-conjugated donkey anti-rabbit IgG (1:200) was incubated at room temperature diluted in PBS 1× 0.1% Triton X-100. The cells were then washed and incubated for 10 min in the dark with propidium iodide (1:500) at 4°C to visualize the nuclei. All the preparations were evaluated by the confocal microscope (LSM 5 Pascal software and Axiovert 200 M; Carl Zeiss Meditec GmbH, Jena, Germany).

Measurement of TEER. HCLE cells were grown on 12 mm Transwell® filters (Corning Incorporated, Corning, NY, USA). TEER was determined with an Evom^2 epithelial voltohmmeter (World Precision Instruments, Sarasota, FL, USA). Before each measurement, the Evom^2 was 'zeroed' according to the manufacturer's directions, and the background resistance was determined using cell-free filters. Cells were exposed for 5 min to the nucleotides Ap_4A and UTP, separately, in a concentration of 100 μM. Afterward, the nucleotides were removed and fresh medium were added. Measurements were performed at different times (1, 2, 6 and 24 h), background was subtracted and values were adjusted to ohms multiplied by area (1.12 cm^2) of the Transwell® (Corning Incorporated, Corning, NY, USA) inserts. Experiments were performed in triplicate.

In vivo *experiments*

Animals. All animal care and experimental procedures complied with the ARVO Statement for the Use of Animals in Ophthalmology and Vision Research and with the European Communities Council Directive (86/609/EEC). Studies involving animals are reported in accordance with the ARRIVE guidelines for reporting experiments involving animals (Kilkenny *et al.*, 2010; McGrath *et al.*, 2010). A total of 24 male rabbits were used in the experiments described here.

All the treatments were performed using a rabbit restrainer model 4800P001 (Tecniplast, Milan, Italy). Normotensive New Zealand white rabbits, weighing 2.5 ± 0.5 kg, were kept in individual cages with food and water *ad libitum*. They were

maintained under a controlled 12/12 h light/dark cycles. Ocular health in rabbits was evaluated before and after the instillation of the compounds and the IOP measurements. A Draize eye test, Efron scale and morphological analyses were performed to assess eye drops tolerability. The status of ocular surface was assessed by a Topcon SL-8Z slit lamp microscope (Topcon, Madrid, Spain) during the study. Those animals used for aqueous humour collection were killed with 15 mg·kg^{-1} ketamine combined with 0.25 mg·kg^{-1} medetomidine. Animals used for wholemount experiments were killed with an overdose of sodium pentobarbital (i.v. injection of 100 mg·kg^{-1}; Mebunat; Orion Ltd., Espoo, Finland).

Wholemount corneas. Six rabbits were used for wholemount experiments to evaluate the effect of topical application of Ap_4A (in doses of 10 μM) in ZO-1 distribution. These compounds were topically applied to the cornea in volumes of 10 μL in the inferior conjunctival sac of one eye of each rabbit, for both compound instilled as control treatment. These experiments were performed during 2 days in six animals. After death, eyes were enucleated and corneas were immediately immersed in a fixative solution of 4% paraformaldehyde in PBS 0.1 M at pH 7.4. Then the corneas were washed in PBS for 1 h. The corneas were then permeabilized with PBS 1× 2% Triton X-100, blocked with PBS 1× 2% Triton X-100 normal goat serum (NGS) 10% for 1 h at room temperature and then stained with the primary antibody rabbit anti-ZO-1 (1:125) diluted in PBS 1× 0.2% Triton X-100 and NGS overnight. Following PBS 1× 0.1% Triton X-100 washing, FITC-conjugated goat anti-rabbit IgG (1:200) was incubated at room temperature diluted in PBS 1× 0.1% Triton X-100. The tissue was then washed with PBS 1× three times and incubated for 20 min in the dark in propidium iodide (1:500) at 4°C to visualize the nuclei. Four radial cuts were performed, using sterile-curved dissecting scissors under stereo microscopy and 0.8 mm forceps. Corneas were then mounted in mounting medium slow DC (DPX). All the preparations were evaluated by the confocal microscope (LSM 5 Pascal software and Axiovert 200 M; Carl Zeiss Meditec GmbH).

Effect of Ap_4A on 5-MCA-NAT delivery in rabbit aqueous humour. Eight rabbits were used for HPLC experiments to evaluate the delivery of 5-MCA-NAT [10 mM formulated in isotonic saline containing 1% dimethyl sulfoxide (DMSO; Sigma-Aldrich)] alone, simultaneously applied with Ap_4A (10 μM) ('Ap_4A + 5-MCA-NAT') and 2 h after Ap_4A (10 μM) pretreatment ('Ap_4A/5-MCA-NAT') through the rabbit corneas. The same experiments were performed with the nucleotide UTP, in the same dose of Ap_4A. One dose was tested per rabbit per day for these experiments. One eye was designated for treatment with the compounds, being the contralateral eye used as control and treated with sterile 0.9% NaCl. Volumes of 10 μL for both compounds and control treatments were applied in the inferior conjunctival sac of one eye of each rabbit.

The delivery of 5-MCA-NAT (10 mM) 2 h after Ap_4A (10 μM) pretreatment ('Ap_4A/5-MCA-NAT') was also tested in rabbits in which silencing of $P2Y_2$ receptors was induced by applying a $P2Y_2$ siRNA topically. The nucleotide sequence of the siRNA target site used (5′-AAC CTG TAC TGC AGC ATC CTC-3′) was previously described in our laboratory (Crooke *et al.*, 2009; Martin-Gil *et al.*, 2012). Forty microlitres of the compound was applied in one single eye of each rabbit for four consecutive days (10 nmol suspended in RNase–DNase-free water). The same volume of sterile NaCl 0.9% was instilled in the contralateral eye of each animal. One hour after siRNA instillation, Ap_4A (10 μM) treatment was performed in order to avoid possible interferences between both compounds. Two hours after Ap_4A application 5-MCA-NAT was added. Finally, aqueous humour was sampled after animal anaesthesia. Animals recovered approximately 1 h after the induction of anaesthesia. Aqueous humour was aspirated using a 23 gauge syringe. Then samples were kept for 2 min at 98°C, and centrifuged at 13 000× *g* to remove proteins before analysis by HPLC. Injections of 50 μL were used in the HPLC (see below) and the corresponding peaks were compared with the concentrations topically applied.

Chromatographic procedures. The chromatographic system consisted of a Waters (Milford, MA, USA) 1515 isocratic HPLC pump, a 2487 dual-absorbance detector and a Reodyne injector, all managed by the Breeze software from Waters. Analysis was performed under ion-pair chromatography conditions by equilibrating the chromatographic system with the mobile phase: 40% methanol, 60% water. The column was a NovaPak C-18 (15 cm length, 0.4 cm diameter; Waters). The flow rate was 0.8 mL min^{-1} and the eluent was monitored at 244 nm wavelength (Andres-Guerrero *et al.*, 2009).

IOP measurements. IOP was measured in 10 rabbits by means of a Tono-Pen XL contact tonometer (Mentor Massachusetts Inc., Norwell, MA, USA) placing the animals in rabbit restrainers as indicated above, being the most appropriate for measuring IOPs within the range of 3–30 mmHg in rabbits (Abrams *et al.*, 1996). Because the application of the tonometer may produce discomfort in the rabbits, a topical anaesthetic (Colicursí double anaesthetic, 0.1 mg mL^{-1} tetracaine plus 0.4 mg mL^{-1} oxybuprocaine in 0.9% saline, diluted 1:3 in 0.9% saline) was applied (10 μL) to the cornea before each measurement of IOP was made (Pintor *et al.*, 2001).

Ten rabbits were used for IOP experiments to evaluate the effect of 1 μM 5-MCA-NAT alone, simultaneously applied with 10 μM of Ap_4A (Ap_4A + 5-MCA-NAT) and 2 h after 10 μM Ap_4A pretreatment (Ap_4A / 5-MCA-NAT), all of them applied in a volume of 10 μL. P2Y receptor antagonists were applied 30 min before the application of Ap_4A. In the case of the $P2Y_2$ siRNA, it was applied in a volume of 40 μL during four consecutive days, once a day. As a control saline 0.9% was used. The IOP was measured twice, 30 min apart, before application of the compounds. After compound instillation, IOP was measured at 30 min and every hour to a maximum of 8 h to study the effect. Animals for pharmacological and nucleotide experiments were used once a week to allow them to recover for the next application. Rabbits used for IOP experiments using siRNA treatments were discarded after the application of the silencing agent. Animals used for aqueous humour studies were not used for IOP experiments after 2 weeks of recovery.

P2Y receptor antagonists and siRNA experiments. Three purinoceptor antagonists were used, PPADS, suramin and RB-2, to investigate the involvement of P2Y receptors. These com-

pounds were applied at 100 μM, 30 min before the application of Ap_4A (at a maximal dose of 10 μM in 10 μL). The contralateral eye received the same volume of vehicle, and it was taken as the control value.

We determined the effects of silencing $P2Y_2$ receptors of New Zealand rabbit eyes by applying the siRNA topically. In eight rabbits, siRNA was applied to the cornea in one single eye along four consecutive days (10 nmol suspended in RNase–DNase-free water, 40 $\mu L \cdot day^{-1}$). The contralateral eyes were used as controls and treated with sterile 0.9% NaCl or a scramble siRNA at the same concentration as described above. IOP experiments and aqueous humour collection were performed following a blind design. For siRNA we used the sequences and the protocols presented elsewhere (Martin-Gil *et al.*, 2012).

Data analysis

Statistical comparisons of treated and non-treated control cells and animals were performed using the one-way ANOVA test. All the statistical analyses were performed using InStat3 software (GraphPad Software, La Jolla, CA, USA). Differences were considered significant when *P*-values < 0.05.

Materials

The dinucleotide Ap_4A, the ERK inhibitor U0126, the P2Y receptor antagonists, pyridoxal phosphate-6-azo (benzene-2′,4′-disulfonic acid) (PPADS), suramin and reactive blue 2 (RB2) were purchased from Sigma-Aldrich (St. Louis, MO, USA). Acrylamide-bisacrylamide, nitrocellulose membranes and prestained molecular weight markers (Precision Protein Standards) were from Bio-Rad (Alcobendas, Madrid, Spain), and the ECL detection system was from GE Healthcare (Barcelona, Spain). The jetPRIME transfection reagent was obtained from Polyplus transfection S.A. (Madrid, Spain). 5-methoxycarbonylamino-N-acetyltryptamine (5-MCA-NAT) was obtained from Tocris (Bristol, UK). Ketamine was purchased from Richter Pharma AG (Wels, Austria). Medetomidine was obtained from Orion Pharma (Madrid, Spain). Colicursí Double Anaesthetic was obtained from Cusí Labs (Barcelona, Spain). Mounting medium slow DC (DPX) was obtained from Panreac (Madrid, Spain). Rabbit anti-ZO-1, anti-occludin and anti-claudin-7 polyclonal antibodies were purchased from Invitrogen (Carlsbad, CA, USA). Mouse monoclonal antibodies GAPDH, pERK1/2 and ERK2 were from Santa Cruz Biotechnology (Santa Cruz, CA, USA). The IgG-HRP secondary antibodies were purchased from Jackson Immunoresearch (West Grove, PA, USA). The rabbit anti-$P2Y_2$ receptor antibody was purchased from Alomone Labs (Jerusalem, Israel) and $P2Y_2$ receptor siRNA was obtained from Dharmacon (Lafayette, CO, USA). $P2Y_2$ siRNA for *in vivo* experiments was obtained from Applied Biosystems (Foster City, CA, USA).

Results

Effect of Ap_4A on ZO-1, occludin and claudin-7 protein levels in HCLE

Pretreatment for 5 min with Ap_4A of the HCLE confluent monolayers resulted in a decrease in the TJ protein levels, compared with the control cells in the absence of the dinucleotide. The highest reduction was found at 2 h [% reduction: ZO-1 (39 ± 8%), occludin (47 ± 8%) and claudin-7 (43 ± 5%)] when compared with non-treated (control) cells ($P < 0.01$, $n = 4$) (Figure 1).

Effect of Ap_4A and UTP on ZO-1 localization in HCLE

Immunocytochemical studies were performed on HCLE cells detecting the presence of ZO-1 in order to see whether the changes detected by Western blot 2 h after the application of the nucleotide were also visible by confocal microscopy. As it can be observed in Figure 2, the typical localization of ZO-1 labelling, all the cell membranes were clearly visible when the cell culture was untreated (Figure 2, upper panels). On the other hand, the application of 100 μM Ap_4A, or UTP, clearly disrupted ZO-1 labelling, as it is shown in Figure 2 (middle and lower panels respectively).

Analysis of TEER

The effect of the exposure to the dinucleotide Ap_4A on paracellular barrier function provided by TJs of HCLE cells was assessed by TEER measurements (Figure 3). One hour after Ap_4A treatment TEER values significantly reduced by 44% as compared with control levels ($P < 0.01$, $n = 4$). Lower TEER values, indicative of an increase in corneal barrier permeability, were measured at longer times of incubation after Ap_4A treatment. Thus, 68 and 52% reduction as compared with control were detected at 2 and 4 h respectively ($P < 0.001$, $n = 4$). After 6 h, TEER values started to progressively return to control values. When HCLE cells were treated with UTP, the mononucleotide showed a similar effect than that induced by Ap_4A, reducing TEER values as compared with the control.

Effect of Ap_4A on ERK1/2 phosphorylation

Apart from modifying TJ protein levels, treatment with Ap_4A induced the activation of ERK1/2 (Figure 4A). Thus, a significant increase in phosphorylation was observed after Ap_4A treatment as compared with the control at all the studied times. The maximal increase was obtained 2 h after the treatment of Ap_4A, changing the values from 115% (control at 2 h) to 371% ($P < 0.001$, $n = 4$) (Figure 4B).

Involvement of $P2Y_2$ receptors and the ERK1/2 pathway in the effects of Ap_4A on TJ proteins

On the corneal epithelium, it has been previously demonstrated that Ap_4A actions such as stimulation of corneal wound healing are mediated by activation of $P2Y_2$ receptors, linked to ERK1/2 activation (Mediero *et al.*, 2008). To elucidate whether $P2Y_2$ receptors and subsequent ERK1/2 activation were also implicated in Ap_4A effect on TJ proteins, a siRNA targeting $P2Y_2$ receptor was used (Figure 5A). As expected, 2 h after Ap_4A treatment ERK1/2 phosphorylation increased by 69% when compared with control and TJ protein levels decreased 35 ± 7% for ZO-1, 26 ± 5% for occludin and 48 ± 4% for claudin-7; these values returning to values close to controls when the siRNA was present ($n = 4$, Figure 5B). These results indicate that $P2Y_2$ stimulation coupled with ERK1/2 activation did mediated the effects of Ap_4A effect on TJ proteins.

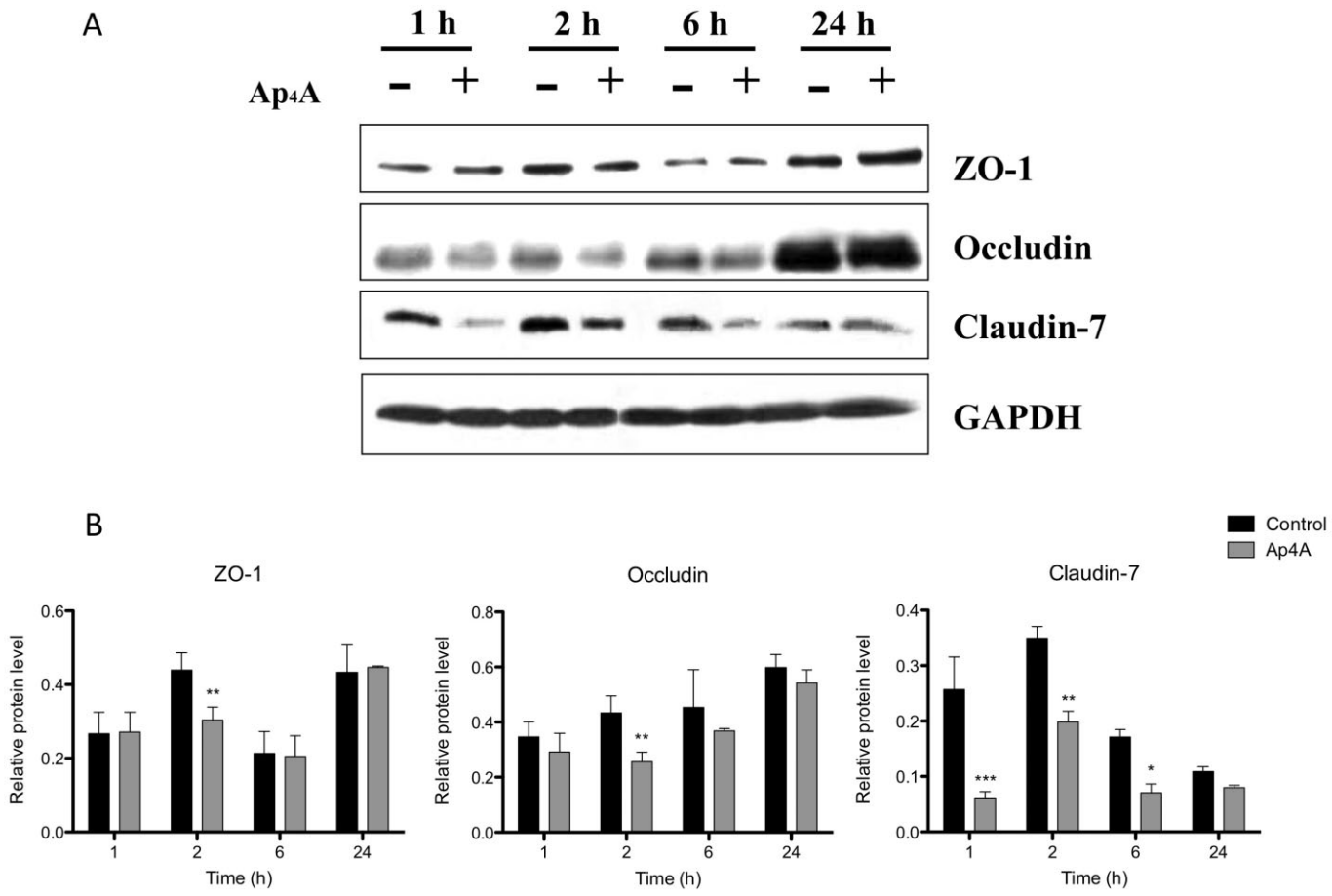

Figure 1

Ap_4A effect on TJ protein levels in HCLE cells. (A) Western blot analysis showing that exposure to Ap_4A (100 μM) decreased TJ protein levels in HCLE cells at different times (1, 2, 6 and 24 h). The Western blot signal was quantified by densitometry. GAPDH served as a loading control. (B) Relative quantification of the Western blot band intensities. Values are the mean ± SD of three independent experiments. *$P < 0.05$, **$P < 0.01$ and ***$P < 0.001$ versus control.

In addition, when cells were pre-incubated with the MEK inhibitor U0126 ($n = 4$, Figure 6), the effect of Ap_4A on ERK1/2 activation and TJ protein levels was abolished. Thus, cells pretreated with MEK inhibitor exhibited TJ protein levels comparable with control (untreated) cells. These results confirmed the role of the ERK1/2 pathway in Ap_4A-induced TJ protein levels reduction.

Distribution of ZO-1 after ocular topical application of Ap_4A

To evaluate the effect of Ap_4A on TJ assembly *in vivo*, immunohistochemistry of ZO-1 was performed in untreated rabbit corneas and after topical application of Ap_4A. In untreated rabbit corneas, ZO-1 immunoreactivity appeared as a continuous line along the regions of cell–cell contact (Figure 7). This immune staining pattern in cell boundaries is a characteristic of TJ in corneal epithelial cells (Ryeom *et al.*, 2000). Topical application of Ap_4A led to changes in ZO-1 distribution. A disruption in the continuous line of ZO-1 staining was seen at the cell borders 2 h after Ap_4A treatment ($n = 4$).

Delivery of 5-MCA-NAT to the anterior chamber of the eye

In order to study whether the effect induced by Ap_4A on TJ protein levels and function could facilitate the entrance of drugs *in vivo*, the delivery of the compound 5-MCA-NAT was examined. Animals were treated with 5-MCA-NAT alone (10 mM, 10 μL), 5-MCA-NAT together with Ap_4A (10 μM, 10 μL) and finally Ap_4A and 2 h later 5-MCA-NAT. The delivery of 5-MCA-NAT 2 h after Ap_4A pretreatment was also tested in rabbits in which silencing of $P2Y_2$ receptors was induced by applying a $P2Y_2$ siRNA topically, as described.

As shown in Figure 8, following topical application, 5-MCA-NAT was detected in the aqueous humour of the rabbit ($n = 4$, Figure 8A). The concentration measured was 97.5 ± 5.3 nM, which was very close to that obtained when Ap_4A was simultaneously applied with 5-MCA-NAT, (105.1 ± 8.69 nM). Interestingly, when Ap_4A was applied 2 h before 5-MCA-NAT, the concentration of the latter was 314.4 ± 10.64 nM. Similarly, the same experiments were performed using UTP 2 h before 5-MCA-NAT, the concentration of the latter being 306.70 ± 8.90 nM (UTP/5-MCA-NAT). When UTP

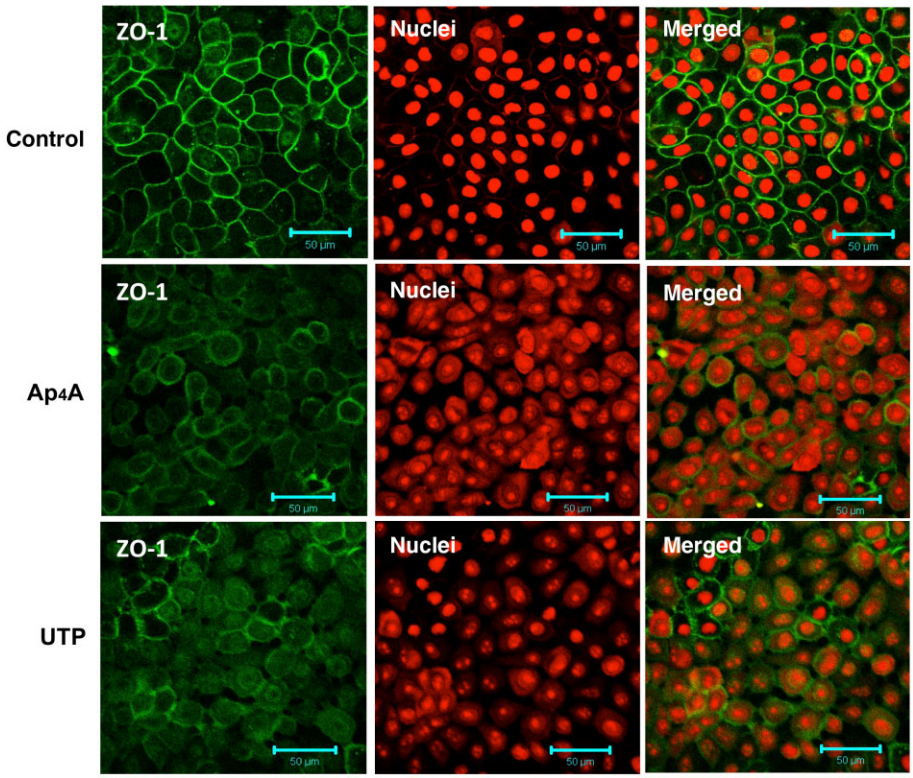

Figure 2

Effect of Ap_4A and UTP on ZO-1 in HCLE cells. Immunocytochemical analysis of ZO-1 in HCLE cells, untreated (upper panels), treated with Ap_4A (middle panels) and treated with UTP (lower panels), visualized 2 h after the application of the corresponding agent. ZO-1 is labelled in green while nuclei were stained with propidium iodide (red). These are representative photographs of three independent experiments.

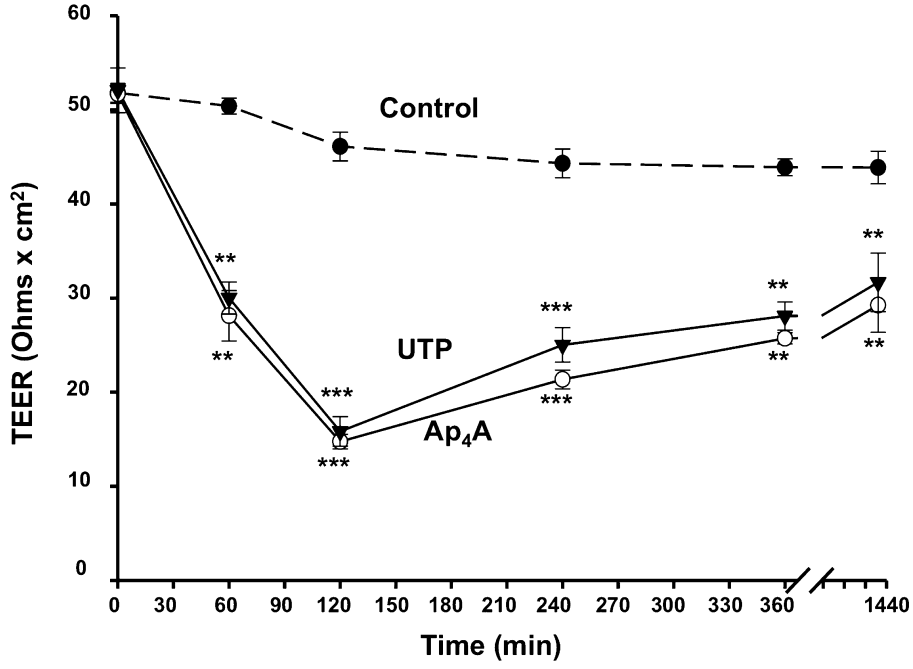

Figure 3

Changes in electrical resistance in HCLE cells after Ap_4A and UTP treatment. TEER measurements were taken at different times (1, 2, 4, 6 and 24 h) after Ap_4A and UTP treatment (both at 100 µM). Values are the mean ± SD of four independent experiments. $^{**}P < 0.01$ at $t = 1$, 6, 24 h and $^{***}P < 0.001$ at $t = 2$ h and $t = 4$ h versus control.

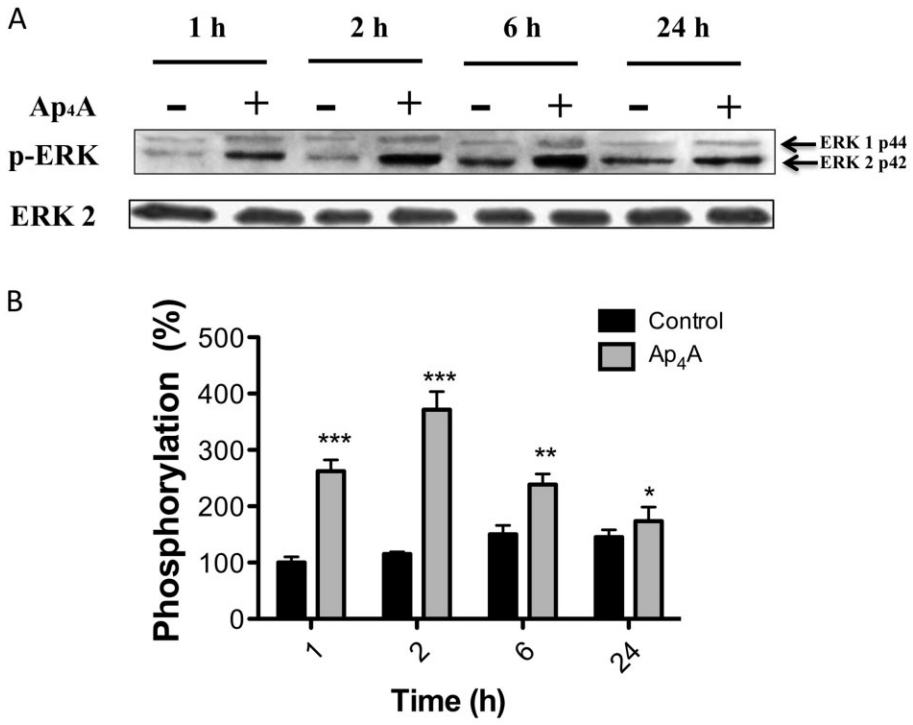

Figure 4

ERK1/2 activation affects TJ protein levels in HCLE cells. (A) Exposure to Ap_4A (100 μM) increased ERK1/2 activation, as analysed by Western blot at different times (1, 2, 6 and 24 h). The Western blot signal was quantified by densitometry. ERK2 served as a loading control. (B) Relative quantification of the Western blot band intensities. Values are the mean ± SD of four independent experiments. *P < 0.05, **P < 0.01 and ***P < 0.001 versus control.

and 5-MCA-NAT were applied simultaneously (UTP + 5-MCA-NAT), the concentration obtained for 5-MCA-NAT was 110.40 ± 11.30 nM. In the presence of the $P2Y_2$ siRNA, the concentration of 5-MCA-NAT was 109.4 ± 6.73 nM (P < 0.001, n = 4) (Figure 8B).

Effects of 5-MCA-NAT and Ap_4A on IOP

The ability of the compound 5-MCA-NAT to reduce IOP was tested at a single dose of 1 μM (10 μL) in New Zealand white rabbits (n = 8). Under this condition IOP reduction was 15.3 ± 3.2%, when compared with the contralateral eye treated with vehicle (saline 0.9%) (Figure 9A).

When the dinucleotide Ap_4A was tested (10 μM, 10 μL) in its ability to reduce IOP in the same animal model (n = 8), the reduction observed was 10.7 ± 1.4% compared with control (Figure 9B).

Combined effects of Ap_4A and 5-MCA-NAT on IOP

Once the hypotensive action of both 5-MCA-NAT and Ap_4A was independently studied, the application of both compounds was investigated. We performed two approaches: on the one hand, simultaneous application of both compounds, and, on the other hand, the application of the dinucleotide Ap_4A, 2 h before the application of 5-MCA-NAT.

The simultaneous application of Ap_4A and 5-MCA-NAT (10 and 1 μM, respectively, in 10 μL) produced a reduction in IOP that was 14.0 ± 2.2% (n = 8), and which returned slowly towards initial values (Figure 10A).

When the experiment was repeated by applying first Ap_4A (10 μM, 10 μL), and 2 h after the melatonin analogue 5-MCA-NAT (1 μM, 10 μL), it was possible to observe a reduction of 23.5 ± 3.6% (n = 8) in IOP compared with control (Figure 10A). Interestingly, rather than returning IOP towards the initial values, IOP remained continuously low during the experimental period.

Concentration–response effect of Ap_4A on the hypotensive effect of 5-MCA-NAT

Because the effect of the pretreatment with Ap_4A 2 h before the topical application of 5-MCA-NAT was very clear and it could be concentration dependent, the ability of different concentrations of the dinucleotide on the hypotensive effect of 5-MCA-NAT was investigated.

A fixed dose of 1 μM (10 μL) of 5-MCA-NAT was assayed in the presence of graded concentrations of Ap_4A ranging from 0.1 to 500 μM, applied 2 h before the melatonin analogue was instilled. As it can be seen in Figure 10B, it was possible to observe a sigmoidal response curve that provided a pD2 value of 5.67 ± 0.16, which corresponded to an EC_{50} value of 2.6 μM (n = 8).

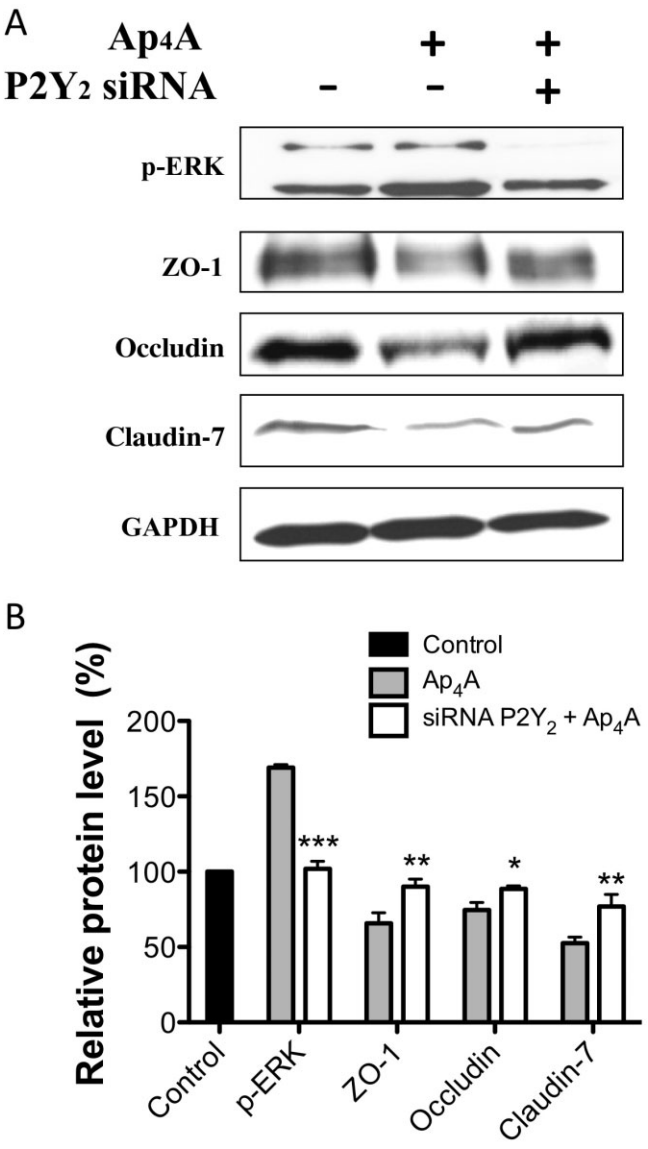

Figure 5

Involvement of $P2Y_2$ receptors in the effects of Ap_4A on TJ proteins. (A) Western blot analysis showing the effects of Ap_4A (100 μM) and the $P2Y_2$ siRNA (50 nM) on ERK1/2 activation and TJ protein levels in HCLE cells. The Western blot signal was quantified by densitometry. GAPDH served as a loading control. (B) Relative quantification of the Western blot band intensities. Values are the mean ± SD of four independent experiments. $^*P < 0.05$, $^{**}P < 0.01$ and $^{***}P < 0.001$ versus control.

Effect of P2Y receptor antagonists and $P2Y_2$ siRNA on Ap_4A effect

Because diadenosine tetraphosphate is a dinucleotide that activates P2Y purinergic receptors, some P2Y receptor antagonists were assayed at a single dose of 100 μM (10 μL), in order to see whether or not the effect Ap_4A produced on 5-MCA-NAT was abolished. As it can be seen in Figure 11, none of the antagonists were able to fully antagonize the effect elicited by Ap_4A. Nevertheless, RB2 and suramin were more effective inhibitors than PPADS, of the potentiation by Ap_4A of the

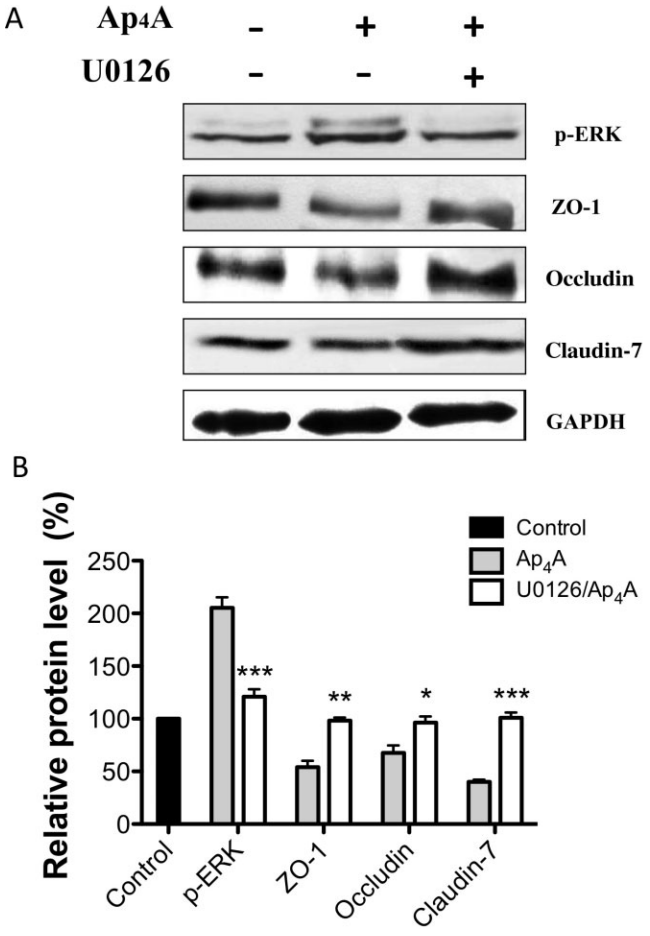

Figure 6

Involvement of ERK1/2 pathway in Ap_4A effect on TJ proteins. (A) Western blot analysis showing the effects of Ap_4A (100 μM) and the MEK inhibitor U0126 (100 μM) on ERK1/2 activation and TJ protein levels in HCLE cells. The Western blot signal was quantified by densitometry. GAPDH served as a loading control. (B) Relative quantification of the Western blot band intensities. Values are the mean ± SD of four independent experiments. $^*P < 0.05$, $^{**}P < 0.01$ and $^{***}P < 0.001$ versus control.

5-MCA-NAT hypotensive effect. RB-2 abolished the effect of Ap_4A to 11.4 ± 0.2%, while suramin effect was 11.5 ± 5.2% (control value in the absence of the antagonists 24.3 ± 2.5%). The effect of PPADS was to reduce the Ap_4A effect to 17.1 ± 3.4% when compared with the effect of 5-MCA-NAT after the treatment of 10 μM Ap_4A ($n = 8$, Figure 11).

Because the pharmacological analysis with the P2Y receptor antagonists was not very conclusive, we decided to study the involvement of the $P2Y_2$ receptor, using a siRNA to silence the expression of this receptor. The application of the siRNA for the $P2Y_2$ receptor abolished Ap_4A-mediated facilitation of the hypotensive action of 5-MCA-NAT (Figure 11).

Discussion

The present work describes the ability of the agonist diadenosine tetraphosphate to modify the permeability of the cornea

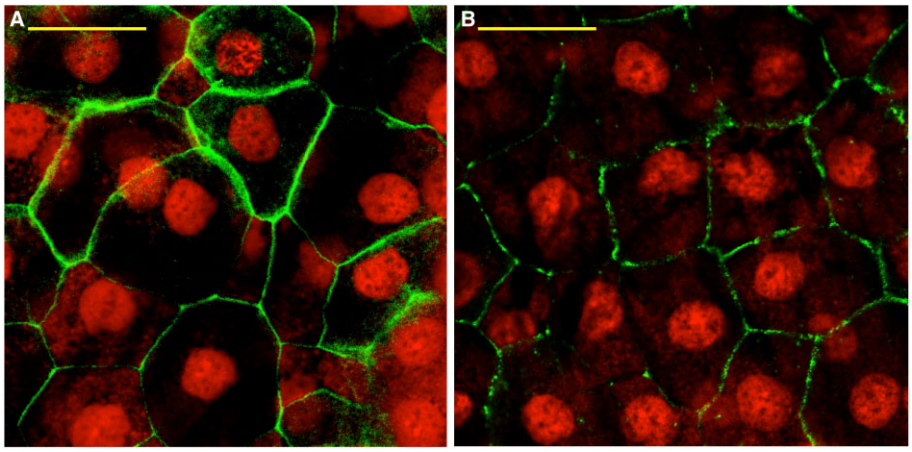

Figure 7

Wholemount preparations stained for ZO-1 after Ap_4A treatment in the corneal epithelium of New Zealand white rabbits. (A) Visualization of the ZO-1 expression in the rabbit corneal epithelium (shown in green) and its combination with propidium iodide to visualize the nuclei (shown in red). These are representative pictures of three independent experiments. (B) Visualization of the ZO-1 expression in the rabbit corneal epithelium (shown in green) and its combination with propidium iodide to visualize the nuclei (shown in red) after treatment with Ap_4A (10 μM).

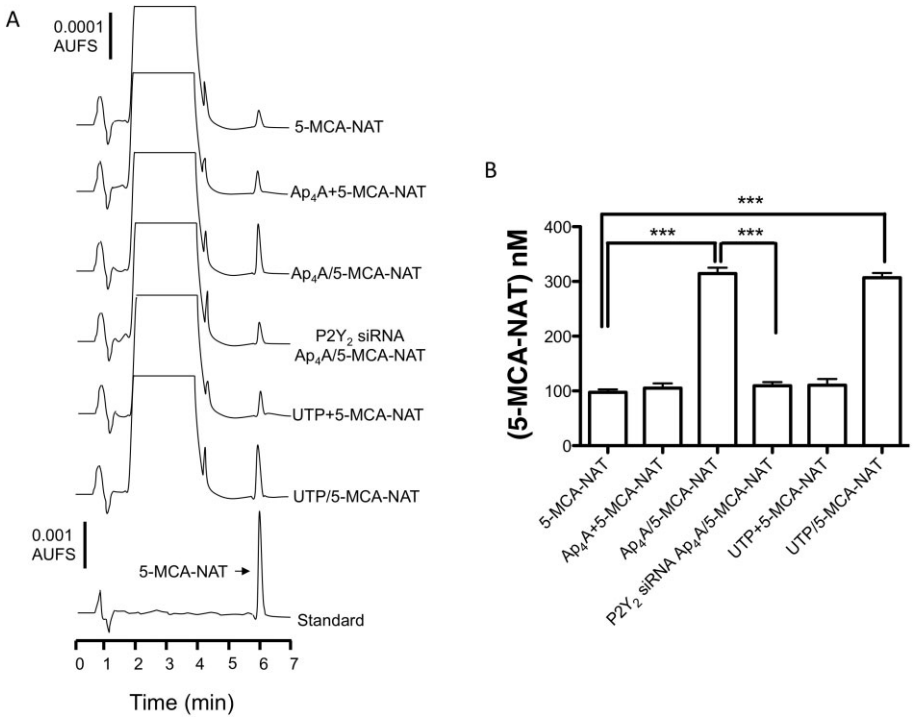

Figure 8

Delivery of 5-MCA-NAT alone, simultaneously combined with Ap_4A (Ap_4A + 5-MCA-NAT) and UTP (UTP + 5-MCA-NAT), applied 2 h after the nucleotide treatment (Ap_4A/5-MCA-NAT, UTP/5-MCA-NAT) and in the presence of $P2Y_2$ siRNA. (A) HPLC elution profiles of the rabbit aqueous humour under the conditions described in Methods. (B) Quantification of the chromatograms described in panel A. Values are the mean ± SD of four independent experiments ***$P < 0.001$ versus control.

to agents able to reduce IOP, such as the melatonin analogue, 5-MCA-NAT. The effect of the dinucleotide was mediated by means of $P2Y_2$ receptors present in the corneal epithelial cells according to the effect of antagonists and $P2Y_2$ siRNA.

The effect of the dinucleotide permitting the entrance of the melatonin analogue 5-MCA-NAT is due to a temporary reduction in the expression of at least some of the proteins forming corneal TJs such as ZO-1, occludin and claudin-7.

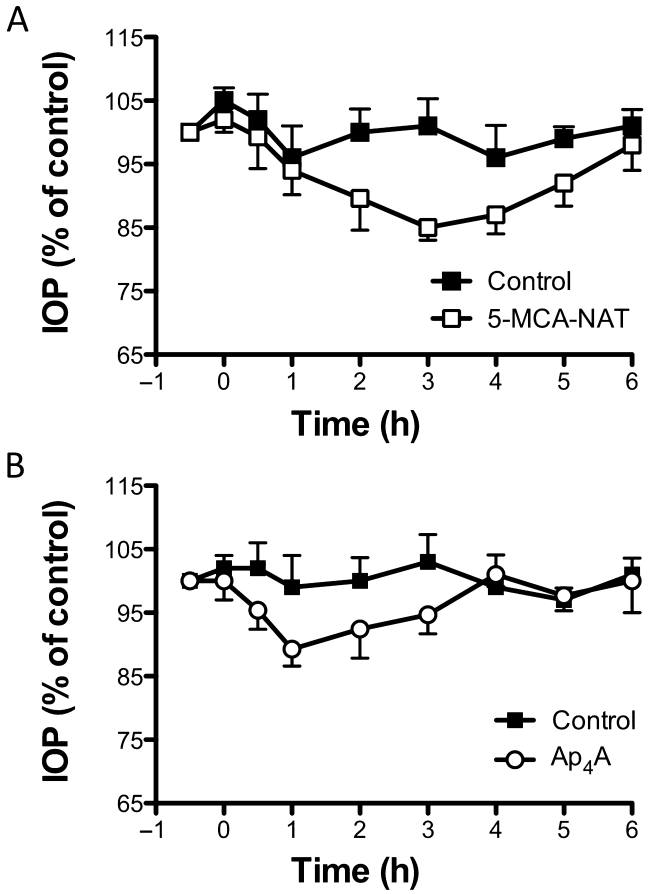

Figure 9

Effects of Ap_4A and 5-MCA-NAT on IOP. (A) Effect of 5-MCA-NAT (1 μM, 10 μL) on IOP in New Zealand White rabbits over 6 h. The values are the mean ± SD of eight independent experiments (100% IOP corresponds to 13.8 ± 3.8 mmHg). (B) Effect of Ap_4A (10 μM, 10 μL) on IOP in New Zealand White rabbits along 6 h. The values are the mean ± SD of eight independent experiments.

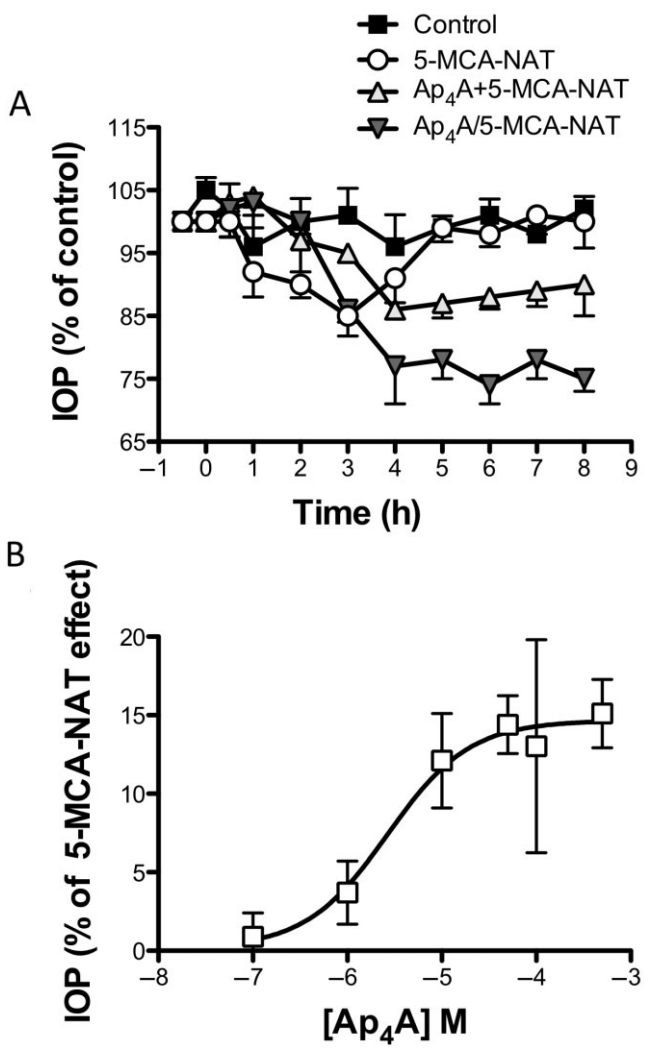

Figure 10

Combined effect of 5-MCA-NAT with Ap_4A on IOP. (A) Effect of 5-MCA-NAT alone (1 μM), 5-MCA-NAT simultaneously combined with Ap_4A (10 μM) (Ap_4A + 5-MCA-NAT) and 5-MCA-NAT applied 2 h after the Ap_4A treatment (Ap_4A/5-MCA-NAT) on IOP in New Zealand White rabbits for 8 h. The values are the mean ± SD of eight independent experiments (100% IOP corresponds to 14.2 ± 3.4 mmHg). (B) Concentration–response curve for Ap_4A (0.1–500 μM) and 5-MCA-NAT (1 μM) 2 h after on IOP in New Zealand White rabbits. The values are the mean ± SD of eight independent experiments.

This reduction in the expression of TJ components induces TJ assembly disruption and a concomitant decrease in TJ barrier function as revealed by measurement of TEER. TEER value is inversely proportional to the permeability of TJs and, certainly, our results of HPLC and physiological studies (IOP) confirmed the increase of corneal epithelial permeability induced by Ap_4A treatment.

The effect of Ap_4A is transitory and was maximal 2 h after the application of the dinucleotide. TJs prevent the entrance of high MW molecules and microorganisms into the eye, allowing a minimal entrance for the delivery of pharmaceutical products by means of the paracellular pathway. This way of access severely limits the entrance of substances, which when topically applied are drained by the lachrymal point instead, reducing the delivery of any given compound inside the eye (Kompella *et al.*, 2010).

This 'window of time' without the barrier effect will facilitate the entrance of substances that under normal conditions have difficulties to be delivered inside the eye. In particular, the compound we have tested here, 5-MCA-NAT, is known to exert a hypotensive effect, reducing IOP in rabbits and monkeys (Pintor *et al.*, 2001; 2003a; Serle *et al.*, 2004). The hypotensive action of this compound is mediated by an unidentified melatonin receptor classically named MT_3 (Pintor *et al.*, 2003a). 5-MCA-NAT regulates chloride efflux, which is one of the most important ions regulating aqueous humour production. Moreover, 5-MCA-NAT can also modify the expression of ciliary adrenoceptors (Crooke *et al.*, 2013). However, a limited amount of this compound passes through the cornea and reaches the ciliary body (Alarma-Estrany *et al.*, 2009). By modifying the corneal permeability, we have shown that it is possible to double the amount entering the

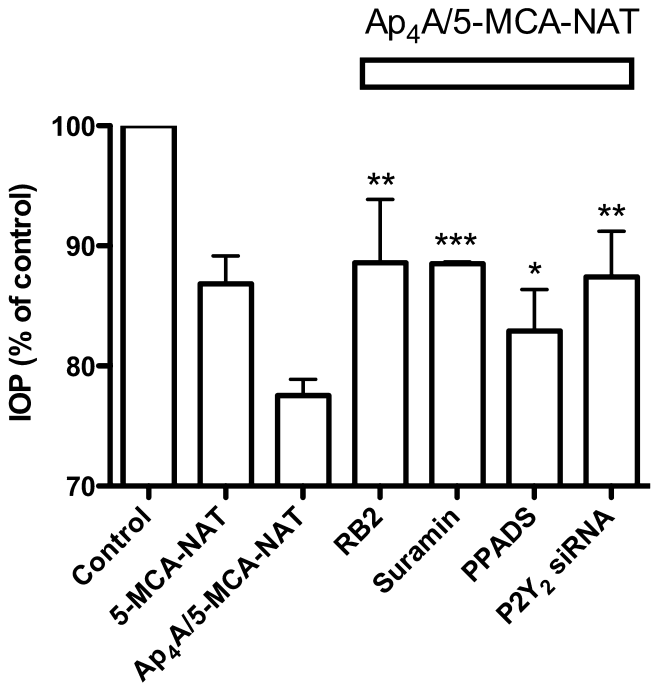

Figure 11

Effect of P2Y receptor antagonists and $P2Y_2$ siRNA on the hypotensive action induced by 5-MCA-NAT applied 2 h after the Ap_4A treatment. The effect of 5-MCA-NAT alone (1 μM), 5-MCA-NAT applied 2 h after the Ap_4A (10 μM) treatment (Ap_4A/5-MCA-NAT) in the absence or in the presence of P2Y receptor antagonists (RB2, suramin and PPADS, all at 100 μM, 10 μL) or $P2Y_2$ siRNA. P2Y receptor antagonists were applied 30 min before the application of Ap_4A. In the case of the $P2Y_2$ siRNA, it was applied in a volume of 40 μL during four consecutive days, once a day before the application of Ap_4A (100% IOP corresponds to 14.4 ± 3.1 mmHg). The values are the mean ± SD of eight independent experiments. $^*P < 0.05$, $^{**}P < 0.01$ and $^{***}P < 0.001$ versus Ap_4A/5-MCA-NAT.

eye , which allowed us to obtain a more robust effect with the application of less 5-MCA-NAT .

An important point to take into account is the time when the dinucleotide is applied. Simultaneous application of the melatonin analogue and Ap_4A did not increase the entry of 5-MCA-NAT and there was no consequent, stronger effect on IOP. Only when there is a delay of 2 h between Ap_4A and 5-MCA-NAT applications, changes in the permeability occur and a more robust physiological effect on IOP is measurable. This suggests that after the $P2Y_2$ receptors are activated, an intracellular mechanism starts which takes time (about 2 h) to have a noticeable effect, in terms of increased passage of 5-MCA-NAT. From the present results, the intracellular signalling pathway involved in this action is ERK1/2 activation, as observed in Western blots and confirmed by the application of U0126 inhibitor. The ERK1/2 signalling pathway has been previously implicated in regulation of TJs by diverse stimuli. This signalling pathway modulates paracellular transport through up- or down-regulation of TJ proteins and consequent changes in TJ assembly and paracellular barrier function. Various growth factors (Feldman *et al.*, 2007), the cytokine IL-17 (Kinugasa *et al.*, 2000), bile (Yang *et al.*, 2005) and thiol compounds (Usatyuk *et al.*, 2006), have been shown to activate ERK1/2 and to increase the barrier function of TJs. On the other hand, ERK1/2 activation has also been involved in the disruption of TJs triggered by oxidative stress (Krizbai *et al.*, 2005), metalloproteinases (Tan *et al.*, 2005), growth factors (Ogawa *et al.*, 2012) and cytokines (Petecchia *et al.*, 2012). These findings indicate that activation of the ERK1/2 pathway can lead to the assembly or disassembly of TJs depending on the stimulus and cell type. In agreement with our results, activation of the ERK1/2 pathway has also been related to TJ disruption in SV40-immortalized corneal epithelial cells (Wang *et al.*, 2004). Furthermore, these authors demonstrated that PKC activation resulted in ERK phosphorylation, which in turn disturbs TJ assembly and barrier function. This is an interesting point as the PLC/PKC pathway is a classical pathway linked to $P2Y_2$ receptor activation in most of the tissues including the eye (Guzman-Aranguez *et al.*, 2013). Thus, Ap_4A-induced $P2Y_2$ receptor activation stimulated the ERK cascade in a way that is dependent on PLC/PKC activation in rabbit corneal epithelial cells (Mediero *et al.*, 2011). Additionally, a possible cross-talk between $P2Y_2$ receptor and receptor tyrosine kinases, leading to ERK activation, has also been suggested (Mediero *et al.*, 2008). Therefore, both PKC-dependent and tyrosine kinase-dependent signalling mechanisms could contribute to link Ap_4A-induced $P2Y_2$ receptor stimulation to ERK activation resulting in TJ disruption. In particular, ERK activation could increase TJ protein endocytosis and subsequent degradation, as reported in other epithelial cell lines (Ikari *et al.*, 2011; Chen *et al.*, 2000).

One of the most important aspects of the present work is the possible application for the pharmaceutical industry. Many of the ways to introduce pharmaceutical compounds within the eye were based in the use of liposomes or even intraocular delivery systems. The possibility of modifying the activity of TJs and therefore the facilitation of the delivery of substances may change the way the topical application of ocular medicines will be applied. It is anyway necessary to perform experiments with typical intraocular drugs such glaucoma treatments to fully confirm the extent and potential of this delivery strategy.

In summary, the dinucleotide Ap_4A can modify temporarily the integrity of the TJs, facilitating the entrance of compounds into the eye. Thus, Ap_4A application can contribute to improving ocular drug delivery and consequently therapeutic efficiency. More work is necessary to investigate which ocular drugs could benefit from increased ocular delivery by means of this mechanism.

Acknowledgements

The authors thank Dr. Ilene Gipson, Schepens Eye Research Institute, Massachusetts Eye and Ear, Harvard Medical School, Boston, MA, USA, for providing the HCLE cells. This work was supported by grants from Ministerio de Ciencia e Innovación (SAF2010-16024 and SAF2013-44416-R) and RETICS (RD12/0034/0003). P. L. and M. J. P. L. are recipients of UCM and FPI grants respectively.

Author contributions

P. L. performed *in vitro* experiments (immunos, Western blot, siRNA). A. G.-A. carried out *in vitro* experiments (TEER, Western blot, writing). M. J. P. L. was responsible for *in vivo* experiments (IOP measurements, siRNA). J. P. was involved in *in vivo* studies (HPLC analysis, writing and editing).

Conflict of interest

None.

References

Abrams LS, Vitale S, Jampel HD (1996). Comparison of three tonometers for measuring intraocular pressure in rabbits. Invest Ophthalmol Vis Sci 37: 940–944.

Adamson RH, Liu B, Fry GN, Rubin LL, Curry FE (1998). Microvascular permeability and number of tight junctions are modulated by cAMP. Am J Physiol 274 (6 Pt 2): H1885–H1894.

Alarma-Estrany P, Crooke A, Pintor J (2009). 5-MCA-NAT does not act through NQO2 to reduce intraocular pressure in New-Zealand white rabbit. J Pineal Res 47: 201–209.

Alexander SPH, Benson HE, Faccenda E, Pawson AJ, Sharman JL, Spedding M *et al* (2013a). The Concise Guide to PHARMACOLOGY 2013/14: Enzymes. Br J Pharmacol 170: 1797–1867.

Alexander SPH, Benson HE, Faccenda E, Pawson AJ, Sharman JL, Spedding M *et al* (2013b). The Concise Guide to PHARMACOLOGY 2013/14: G Protein-Coupled Receptors. Br J Pharmacol 170: 1459–1581.

Andres-Guerrero V, Alarma-Estrany P, Molina-Martinez IT, Peral A, Herrero-Vanrell R, Pintor J (2009). Ophthalmic formulations of the intraocular hypotensive melatonin agent 5-MCA-NAT. Exp Eye Res 88: 504–511.

Balda MS, Gonzalez-Mariscal L, Matter K, Cereijido M, Anderson JM (1993). Assembly of the tight junction: the role of diacylglycerol. J Cell Biol 123: 293–302.

Ban Y, Dota A, Cooper LJ, Fullwood NJ, Nakamura T, Tsuzuki M *et al*. (2003). Tight junction-related protein expression and distribution in human corneal epithelium. Exp Eye Res 76: 663–669.

Basuroy S, Seth A, Elias B, Naren AP, Rao R (2006). MAPK interacts with occludin and mediates EGF-induced prevention of tight junction disruption by hydrogen peroxide. Biochem J 393 (Pt 1): 69–77.

Boucher I, Rich C, Lee A, Marcincin M, Trinkaus-Randall V (2010). The P2Y2 receptor mediates the epithelial injury response and cell migration. Am J Physiol Cell Physiol 299: C411–C421.

Brown RC, Davis TP (2002). Calcium modulation of adherens and tight junction function: a potential mechanism for blood-brain barrier disruption after stroke. Stroke 33: 1706–1711.

Chen Y, Lu Q, Schneeberger EE, Goodenough DA (2000). Restoration of tight junction structure and barrier function by down-regulation of the mitogen-activated protein kinase pathway in ras-transformed Madin-Darby canine kidney cells. Mol Biol Cell 11: 849–862.

Cohen TS, Gray Lawrence G, Khasgiwala A, Margulies SS (2010). MAPK activation modulates permeability of isolated rat alveolar epithelial cell monolayers following cyclic stretch. PLoS ONE 5: e10385.

Crooke A, Mediero A, Guzman-Aranguez A, Pintor J (2009). Silencing of P2Y2 receptor delays Ap4A-corneal re-epithelialization process. Mol Vis 15: 1169–1178.

Crooke A, Huete-Toral F, Martinez-Aguila A, Martin-Gil A, Pintor J (2013). Melatonin and its analog 5-methoxycarbonylamino-N-acetyltryptamine potentiate adrenergic receptor-mediated ocular hypotensive effects in rabbits: significance for combination therapy in glaucoma. J Pharmacol Exp Ther 346: 138–145.

Feldman G, Kiely B, Martin N, Ryan G, McMorrow T, Ryan MP (2007). Role for TGF-beta in cyclosporine-induced modulation of renal epithelial barrier function. J Am Soc Nephrol 18: 1662–1671.

Furuse M, Hirase T, Itoh M, Nagafuchi A, Yonemura S, Tsukita S (1993). Occludin: a novel integral membrane protein localizing at tight junctions. J Cell Biol 123 (6 Pt 2): 1777–1788.

Gipson IK, Spurr-Michaud S, Argueso P, Tisdale A, Ng TF, Russo CL (2003). Mucin gene expression in immortalized human corneal-limbal and conjunctival epithelial cell lines. Invest Ophthalmol Vis Sci 44: 2496–2506.

Guzman-Aranguez A, Crooke A, Peral A, Hoyle CH, Pintor J (2007). Dinucleoside polyphosphates in the eye: from physiology to therapeutics. Prog Retin Eye Res 26: 674–687.

Guzman-Aranguez A, Loma P, Pintor J (2011). Focus on molecules: diadenosine tetraphosphate. Exp Eye Res 92: 96–97.

Guzman-Aranguez A, Santano C, Martin-Gil A, Fonseca B, Pintor J (2013). Nucleotides in the eye: focus on functional aspects and therapeutic perspectives. J Pharmacol Exp Ther 345: 331–341.

Harhaj NS, Antonetti DA (2004). Regulation of tight junctions and loss of barrier function in pathophysiology. Int J Biochem Cell Biol 36: 1206–1237.

Hollande F, Blanc EM, Bali JP, Whitehead RH, Pelegrin A, Baldwin GS *et al*. (2001). HGF regulates tight junctions in new nontumorigenic gastric epithelial cell line. Am J Physiol Gastrointest Liver Physiol 280: G910–G921.

Ikari A, Takiguchi A, Atomi K, Sugatani J (2011). Epidermal growth factor increases clathrin-dependent endocytosis and degradation of claudin-2 protein in MDCK II cells. J Cell Physiol 226: 2448–2456.

Ivanov AI, Samarin SN, Bachar M, Parkos CA, Nusrat A (2009). Protein kinase C activation disrupts epithelial apical junctions via ROCK-II dependent stimulation of actomyosin contractility. BMC Cell Biol 10: 36.

Kilkenny C, Browne W, Cuthill IC, Emerson M, Altman DG (2010). Animal research: Reporting *in vivo* experiments: the ARRIVE guidelines. Br J Pharmacol 160: 1577–1579.

Kinugasa T, Sakaguchi T, Gu X, Reinecker HC (2000). Claudins regulate the intestinal barrier in response to immune mediators. Gastroenterology 118: 1001–1011.

Klingler C, Kniesel U, Bamforth SD, Wolburg H, Engelhardt B, Risau W (2000). Disruption of epithelial tight junctions is prevented by cyclic nucleotide-dependent protein kinase inhibitors. Histochem Cell Biol 113: 349–361.

Kompella UB, Kadam RS, Lee VH (2010). Recent advances in ophthalmic drug delivery. Ther Deliv 1: 435–456.

Krizbai IA, Bauer H, Bresgen N, Eckl PM, Farkas A, Szatmari E *et al*. (2005). Effect of oxidative stress on the junctional proteins of cultured cerebral endothelial cells. Cell Mol Neurobiol 25: 129–139.

Lang JC (1995). Ocular drug delivery conventional ocular formulations. Adv Drug Delivery Rev 16: 39–43.

Martin-Gil A, de Lara MJ, Crooke A, Santano C, Peral A, Pintor J (2012). Silencing of P2Y(2) receptors reduces intraocular pressure in New Zealand rabbits. Br J Pharmacol 165 (4b): 1163–1172.

Martin-Padura I, Lostaglio S, Schneemann M, Williams L, Romano M, Fruscella P *et al*. (1998). Junctional adhesion molecule, a novel member of the immunoglobulin superfamily that distributes at intercellular junctions and modulates monocyte transmigration. J Cell Biol 142: 117–127.

McGrath J, Drummond G, McLachlan E, Kilkenny C, Wainwright C (2010). Guidelines for reporting experiments involving animals: the ARRIVE guidelines. Br J Pharmacol 160: 1573–1576.

Mediero A, Guzman-Aranguez A, Crooke A, Peral A, Pintor J (2008). Corneal re-epithelialization stimulated by diadenosine polyphosphates recruits RhoA/ROCK and ERK1/2 pathways. Invest Ophthalmol Vis Sci 49: 4982–4992.

Mediero A, Crooke A, Guzman-Aranguez A, Pintor J (2011). Phospholipase C/protein kinase C pathway is essential for corneal re-epithelialization induced by Ap(4)A. Curr Eye Res 36: 1108–1115.

Mineta K, Yamamoto Y, Yamazaki Y, Tanaka H, Tada Y, Saito K *et al*. (2011). Predicted expansion of the claudin multigene family. FEBS Lett 585: 606–612.

Ogawa M, Kojima T, Someya M, Nomura K, Takasawa A, Murata M *et al*. (2012). Epidermal growth factor modulates claudins and tight junctional functions in ovarian cancer cell lines. Histochem Cell Biol 138: 323–338.

Pawson AJ, Sharman JL, Benson HE, Faccenda E, Alexander SP, Buneman OP *et al*; NC-IUPHAR (2014). The IUPHAR/BPS Guide to PHARMACOLOGY: an expert-driven knowledge base of drug targets and their ligands. Nucl Acids Res 42 (Database Issue): D1098-1106.

Peral A, Loma P, Yerxa B, Pintor J (2008). Topical application of nucleotides increase lysozyme levels in tears. Clin Ophthalmol 2: 261–267.

Petecchia L, Sabatini F, Usai C, Caci E, Varesio L, Rossi GA (2012). Cytokines induce tight junction disassembly in airway cells via an EGFR-dependent MAPK/ERK1/2-pathway. Lab Invest 92: 1140–1148.

Pflugfelder SC, Farley W, Luo L, Chen LZ, de Paiva CS, Olmos LC *et al*. (2005). Matrix metalloproteinase-9 knockout confers resistance to corneal epithelial barrier disruption in experimental dry eye. Am J Pathol 166: 61–71.

Pintor J, Martin L, Pelaez T, Hoyle CH, Peral A (2001). Involvement of melatonin MT(3) receptors in the regulation of intraocular pressure in rabbits. Eur J Pharmacol 416: 251–254.

Pintor J, Carracedo G, Alonso MC, Bautista A, Peral A (2002a). Presence of diadenosine polyphosphates in human tears. Pflugers Arch 443: 432–436.

Pintor J, Carracedo G, Alonso MC, Bautista A, Peral A (2002b). Presence of diadenosine polyphosphates in human tears. Pflugers Arch 443: 432–436.

Pintor J, Pelaez T, Hoyle CH, Peral A (2003a). Ocular hypotensive effects of melatonin receptor agonists in the rabbit: further evidence for an MT3 receptor. Br J Pharmacol 138: 831–836.

Pintor J, Peral A, Pelaez T, Martin S, Hoyle CH (2003b). Presence of diadenosine polyphosphates in the aqueous humor: their effect on intraocular pressure. J Pharmacol Exp Ther 304: 342–348.

Ryeom SW, Paul D, Goodenough DA (2000). Truncation mutants of the tight junction protein ZO-1 disrupt corneal epithelial cell morphology. Mol Biol Cell 11: 1687–1696.

Sadowska GB, Malaeb SN, Stonestreet BS (2010). Maternal glucocorticoid exposure alters tight junction protein expression in the brain of fetal sheep. Am J Physiol Heart Circ Physiol 298: H179–H188.

Serle JB, Wang RF, Peterson WM, Plourde R, Yerxa BR (2004). Effect of 5-MCA-NAT, a putative melatonin MT3 receptor agonist, on intraocular pressure in glaucomatous monkey eyes. J Glaucoma 13: 385–388.

Sosnova-Netukova M, Kuchynka P, Forrester JV (2007). The suprabasal layer of corneal epithelial cells represents the major barrier site to the passive movement of small molecules and trafficking leukocytes. Br J Ophthalmol 91: 372–378.

Soto D, Pintor J, Peral A, Gual A, Gasull X (2005). Effects of dinucleoside polyphosphates on trabecular meshwork cells and aqueous humor outflow facility. J Pharmacol Exp Ther 314: 1042–1051.

Stamatovic SM, Dimitrijevic OB, Keep RF, Andjelkovic AV (2006). Protein kinase Calpha-RhoA cross-talk in CCL2-induced alterations in brain endothelial permeability. J Biol Chem 281: 8379–8388.

Tan X, Egami H, Abe M, Nozawa F, Hirota M, Ogawa M (2005). Involvement of MMP-7 in invasion of pancreatic cancer cells through activation of the EGFR mediated MEK-ERK signal transduction pathway. J Clin Pathol 58: 1242–1248.

Usatyuk PV, Parinandi NL, Natarajan V (2006). Redox regulation of 4-hydroxy-2-nonenal-mediated endothelial barrier dysfunction by focal adhesion, adherens, and tight junction proteins. J Biol Chem 281: 35554–35566.

Wang Y, Zhang J, Yi XJ, Yu FS (2004). Activation of ERK1/2 MAP kinase pathway induces tight junction disruption in human corneal epithelial cells. Exp Eye Res 78: 125–136.

Wittchen ES, Haskins J, Stevenson BR (1999). Protein interactions at the tight junction. Actin has multiple binding partners, and ZO-1 forms independent complexes with ZO-2 and ZO-3. J Biol Chem 274: 35179–35185.

Yang R, Harada T, Li J, Uchiyama T, Han Y, Englert JA *et al*. (2005). Bile modulates intestinal epithelial barrier function via an extracellular signal related kinase 1/2 dependent mechanism. Intensive Care Med 31: 709–717.

Yoshida Y, Ban Y, Kinoshita S (2009). Tight junction transmembrane protein claudin subtype expression and distribution in human corneal and conjunctival epithelium. Invest Ophthalmol Vis Sci 50: 2103–2108.